





Functionally discrete fine roots differ in microbial assembly, microbial functional potential, and produced metabolites

William L. King^{1,2}  | Caylon F. Yates^{1,3} | Lily Cao^{1,3,4} | Sean O'Rourke-Ibach¹ | Suzanne M. Fleishman^{3,4,5} | Sarah C. Richards^{1,3,6} | Michela Centinari^{3,4} | Benjamin D. Hafner²  | Marc Goebel⁷ | Taryn Bauerle² | Young-Mo Kim⁸ | Carrie D. Nicora⁸ | Christopher R. Anderton⁹  | David M. Eissenstat^{3,5} | Terrence H. Bell^{1,3,6,10} 

¹Department of Plant Pathology and Environmental Microbiology, The Pennsylvania State University, University Park, Pennsylvania, USA

²School of Integrative Plant Science, Cornell University, Ithaca, New York, USA

³Intercollege Graduate Degree Program in Ecology, The Pennsylvania State University, University Park, Pennsylvania, USA

⁴Department of Plant Science, The Pennsylvania State University, University Park, Pennsylvania, USA

⁵Department of Ecosystem Science and Management, The Pennsylvania State University, University Park, Pennsylvania, USA

⁶Intercollege Graduate Degree Program in International Agriculture and Development, The Pennsylvania State University, University Park, Pennsylvania, USA

⁷Department of Natural Resources and the Environment, Cornell University, Ithaca, New York, USA

⁸Biological Sciences Division, Pacific Northwest National Laboratory, Richland, Washington, USA

⁹Environmental Molecular Sciences Laboratory, Pacific Northwest National Laboratory, Richland, Washington, USA

¹⁰Department of Physical & Environmental Sciences, University of Toronto Scarborough, Toronto, Ontario, Canada

Correspondence

William L. King

Email: wlk46@cornell.edu

Terrence H. Bell

Email: terrence.bell@utoronto.ca

Funding information

USDA National Institute of Food and Agriculture; DOE Biological and Environmental Research program; DOE Environmental Molecular Sciences Laboratory; NSF Centre for Research on Programmable Plant Systems

Abstract

Traditionally, fine roots were grouped using arbitrary size categories, rarely capturing the heterogeneity in physiology, morphology and functionality among different fine root orders. Fine roots with different functional roles are rarely separated in microbiome-focused studies and may result in confounding microbial signals and host-filtering across different root microbiome compartments. Using a 26-year-old common garden, we sampled fine roots from four temperate tree species that varied in root morphology and sorted them into absorptive and transportive fine roots. The rhizoplane and rhizosphere were characterized using 16S rRNA gene and internal transcribed spacer region amplicon sequencing and shotgun metagenomics for the rhizoplane to identify potential microbial functions. Fine roots were subject to metabolomics to spatially characterize resource availability. Both fungi and bacteria differed according to root functional type. We observed additional differences between the bacterial rhizoplane and rhizosphere compartments for absorptive but not transportive fine roots. Rhizoplane bacteria, as well as the root metabolome and potential microbial functions, differed between

This is an open access article under the terms of the Creative Commons Attribution License, which permits use, distribution and reproduction in any medium, provided the original work is properly cited.

© 2023 The Authors. *Plant, Cell & Environment* published by John Wiley & Sons Ltd.

absorptive and transportive fine roots, but not the rhizosphere bacteria. Functional differences were driven by sugar transport, peptidases and urea transport. Our data highlights the importance of root function when examining root-microbial relationships, emphasizing different host selective pressures imparted on different root microbiome compartments.

KEYWORDS

microbial functions, rhizoplane, rhizosphere, root microbiome, root order, root physiology, spatial colonization

1 | INTRODUCTION

By releasing carbon (C) resources from their finest roots, plants can influence which microbes are present in direct root surface-associated (i.e., the rhizoplane) and root-adjacent (i.e., the rhizosphere) environments (Edwards et al., 2015; Reinhold-Hurek et al., 2015), often resulting in microbial assemblages that differ from those in the surrounding bulk soil (Bulgarelli et al., 2012; King et al., 2021; Reinhold-Hurek et al., 2015). In many studies of root-associated microbial composition, fine roots are homogenized before microbial sampling (Bulgarelli et al., 2012; Edwards et al., 2015; Fitzpatrick et al., 2018; Fleishman et al., 2022; Hu et al., 2018; Lundberg et al., 2012; Peiffer et al., 2013; Schreiter et al., 2014; Zhang et al., 2017); however, this process of homogenization assumes that all fine roots are equal. Fine roots have substantial structural and functional differences (McCormack et al., 2015), which also impact their microbial associations as well (King et al., 2021).

Traditionally, fine roots have been defined as all roots below an arbitrary diameter, typically 2.0 mm (Holdaway et al., 2011; McCormack et al., 2015; Pregitzer et al., 2002). Unfortunately, this size exclusion approach does not account for the heterogeneity of root physiology, morphology and functionality within a fine root cluster (McCormack et al., 2015; Pregitzer et al., 2002). There are alternative methods for fine root classification which rely on categorization based on branching order or functional role, but these are rarely applied in microbiome-focused studies. When classifying by either branching order (i.e., counting from the most distal roots to the root base) or functional role, fine roots are typically grouped into absorptive fine roots (e.g., root orders 1 and 2) and transportive fine roots (e.g., usually root orders 4 and above) (Fitter, 1982; McCormack et al., 2015; Pregitzer et al., 2002), depending on the species. Absorptive and transportive fine roots are known to differ structurally, for example, by root hair density and morphology (Hishi, 2007; Pregitzer et al., 2002; Valenzuela-Estrada et al., 2008), and functionally, with differences in respiration rate, life span and absorptive capacity (Gu et al., 2011; Guo, Mitchell, et al., 2008; Guo, Xia, et al., 2008; Makita et al., 2009; McCormack et al., 2015; Valenzuela-Estrada et al., 2008). Importantly, fine root size and morphology can vary widely across woody plant species, so classifying fine roots by their expected functional roles (i.e., by

branching root order) can facilitate between-species comparisons (McCormack et al., 2015; Pregitzer et al., 2002).

Functional classification of fine roots has implications that extend beyond root physiology. For instance, absorptive fine roots are considered a “microbial hotspot” of activity (Reinhold-Hurek et al., 2015), supporting greater bacterial abundance and mycorrhizal fungal colonization (Guo et al., 2008b; King et al., 2021), and exerting stronger selective pressures than higher order roots (i.e., transportive fine roots) on microbes in surrounding soil (King et al., 2021). Plants likely apply different degrees of selective pressure between functionally discrete fine roots, which could be mediated by host-provided resources or host-associated engineering of the abiotic environment (e.g., pH changes with hydrogen or hydroxide ion flux (Kuzyakov & Razavi, 2019)). Roots are well known to exert a gradient of influence on their surrounding environment (Kuzyakov & Razavi, 2019), with increasing microbial diversity/richness with increasing distance from the root (Bulgarelli et al., 2012, 2013; Chen et al., 2016; Reinhold-Hurek et al., 2015), but is this the case across different functional root types? For instance, compared to absorptive roots, transportive fine roots have a relatively minor role in water, nutrient and oxygen uptake (Fan & Guo, 2010; Gordon & Jackson, 2000; Hishi, 2007; McCormack et al., 2015; Minerovic et al., 2018; Pregitzer et al., 2002; Segal et al., 2008; Valenzuela-Estrada et al., 2008).

We previously showed that bacterial composition in the ectorrhizosphere (the combination of the rhizoplane and rhizosphere root compartments; defined as the rhizoplane in that study) differed significantly by fine root function, indicating that homogenization could mask microbial signals of interest (King et al., 2021). We did not establish whether this pattern can persist with increasing distance from the fine root surface (i.e., rhizoplane vs. rhizosphere); if so, these fine-scale differences will influence a much larger portion of the environment. Although we suspected that fine-scale assembly patterns were driven by differential resource availability, we did not assess patterns of C release in that study.

Using a 26-year-old common garden forest, we collected fine roots from four temperate tree species that varied widely in morphology and mycorrhizal type and sorted fine roots by root branching order, grouping presumed absorptive roots (i.e., root orders 1 and 2) separately from presumed transportive fine roots

(i.e., root orders 4 and 5). To assess differences in root function and microbial association, we integrated amplicon sequencing (microbial composition), shotgun metagenomics (microbial composition and potential function) and the root metabolome (resource diversity). We combined metabolomics with shotgun metagenomics and amplicon sequencing to investigate whether the metabolites available between root functional types (absorptive vs. transportive) could explain spatial assembly patterns for differing root compartments. As the absorptive fine roots are implicated as the hotspots of root-microbial activity, we hypothesized that (i) fine root physiology (absorptive and transportive) would interact with root microbiome compartment (rhizosphere and rhizoplane) to drive differences in microbial composition, with rhizoplane microorganisms being more strongly affected by root physiology, and (ii) the carbon resources available for each root functional type would differ with a greater abundance of labile carbon resources in absorptive fine roots. Deciphering root-microbial feedback requires an understanding of how plants exert their influence on different root microbiome compartments and how host selective pressures can be dissimilar with spatial scale among functionally discrete fine roots.

2 | MATERIALS AND METHODS

2.1 | Study site

At the Russell E. Larson Agricultural Research Centre (40°42' N, 77°57' W), we sampled a 26-year-old experimental common garden forest, managed by The Pennsylvania State University (Luke McCormack et al., 2012). The common garden forest was established in 1996 with 1-year-old seedlings in a randomized complete block design. Before seedling planting, soil conditions were roughly homogeneous throughout the site. For this study, we chose *Liriodendron tulipifera* L., *Pinus strobus* L., *Acer saccharum* Marshall and *Quercus rubra* L. These tree species were chosen to capture arbuscular mycorrhizal (AM) fungi associating with a thin-root (*A. saccharum*) and a thick-root (*L. tulipifera*) tree species, and ectomycorrhizal (EM) fungi associating with a thin-root (*Q. rubra*) and thick-root (*P. strobus*) tree species (Pregitzer et al., 2002), and to correspond with tree species selected in a previous study (King et al., 2021). Representative images of functionally distinct fine roots are available in a previous study (displayed as figure 1 and Supplementary figure 1 in King et al. [2021]).

2.2 | Root collection

On 30 August 2021, fine roots were collected from three blocks. For each tree species in each block, two root clusters were collected using a spading fork and gently shaken to remove loosely adherent soil. Root order was determined by the topological approach (e.g., Pregitzer et al. [2002] and McCormack et al. [2015]). In the field, we separated the root orders into absorptive and transportive fine roots

using 70% ethanol-washed tools and cutting boards. We defined absorptive fine roots as root orders 1 and 2 (henceforth 'R1/2' or 'absorptive fine roots') and transportive fine roots as root orders 4 and 5 (henceforth 'R4/5' or 'transportive fine roots'). Two subsamples of absorptive and transportive fine roots were collected. Thus, there were a total of six samples of root tissue (three blocks by two subsamples) each for absorptive and transportive roots for each of the four species. One subsample was placed inside a sterile 15-mL tube, washed three times using sterile water and the cleaned roots were placed into a new 15-mL tube and immediately snap-frozen for later metabolomic analyses. The other subsample, destined for DNA-based investigations, was placed into a sterile 15-mL tube, stored on ice and transported to the laboratory for further processing.

2.3 | Processing roots in the laboratory

Roots collected for DNA extraction were separated into the rhizosphere and rhizoplane compartments. To collect the rhizosphere compartment, roots were washed with 5 mL of sterile water and vortexed for 10 s. The soil solution was then pipetted to a new 15-mL tube. Each root sample was washed three times for a total of 15 mL of soil solution. Tubes with the soil solution were then centrifuged at 10 000g for 5 min. The tube was decanted, weighed, resuspended in 1 mL of sterile water, transferred to a 1.5-mL tube and frozen at -20°C until needed. On average, we collected 207 mg of rhizosphere soil from each root sample. To collect the rhizoplane compartment, 5 mL of sterile water was added to the thrice-washed roots and the roots were sonicated six times for 30 s (total of 3 min). Sonication, after root washing, is a common technique to collect the rhizoplane compartment and effectively removes surface-attached microorganisms (Bulgarelli et al., 2012; Edwards et al., 2015). The sonicated roots were then moved to a fresh tube. To ensure we collected as much rhizoplane solution as possible, the sonicated roots were centrifuged at 100g for 30 s to collect excess liquid and the liquid was transferred back into the rhizoplane compartment tube. The rhizoplane compartment tube was centrifuged at 10 000g for 15 min and the top 4 mL of solution was removed. The remaining 1 mL of solution was mixed by pipetting, transferred to a fresh 1.5-mL tube and frozen at -20°C until needed.

2.4 | Metabolomic analysis

Cleaned roots were shipped on dry ice and processed for metabolomic analyses at the US DOE Pacific Northwest National Laboratory (PNNL) and Environmental Molecular Sciences Laboratory. Plant root samples were ground by using a mortar and pestle in liquid nitrogen. Roughly ground samples were lyophilized and ground again using a Geno grinder (SPEX SamplePrep) with 5 mm stainless steel beads to generate fine powder. From each sample, 10 mg was used to extract metabolites using the MPLEx protocol (Nakayasu et al., 2016) and the combined fraction of the polar and 1/3 of the nonpolar layers were transferred into glass vials. The remaining nonpolar lipid layer was stored at -20°C. The protein

interlayer was rinsed with cold methanol, and after centrifugation the supernatant was added to the metabolite sample and dried completely using a speed-vacuum concentrator. The dried metabolite extracts were chemically derivatized based on a previously reported method (Kim et al., 2015). To protect carbonyl groups and reduce the number of tautomeric isomers, methoxyamine (20 μ L of a 30 mg/mL stock in pyridine) was added to each sample, followed by incubation at 37°C with shaking for 90 min. To derivatize hydroxyl and amine groups to trimethylsilylated forms, N-methyl-N-(trimethylsilyl) trifluoroacetamide with 1% trimethylchlorosilane (80 μ L) was added to each vial, followed by incubation at 37°C with shaking for 30 min. Samples were analyzed by gas chromatography-mass spectrometer (GC-MS) coupled with a HP-5MS column (30 m \times 0.25 mm \times 0.25 μ m; Agilent Technologies), which was used for untargeted analyses. We injected 1 μ L of sample into splitless mode and the helium gas flow rate was determined by Retention Time Locking function based on analysis of deuterated myristic acid (Agilent Technologies). The injection port temperature was held at 250°C throughout the analysis. The GC oven was held at 60°C for 1 min after injection, and the temperature was increased to 325°C by 10°C/min, followed by a 10 min hold at 325°C. Data were collected over the mass range 50–600 m/z. A mixture of FAMES (C8–C28) was analyzed together with the samples for retention index alignment purposes during subsequent data analysis. GC-MS data files were converted to CDF format and then deconvoluted and aligned by Metabolite Detector (Hiller et al., 2009). Identification of metabolites was done by matching with the PNNL in-house metabolomics database augmented from the Fiehn database (Kind et al., 2009). The database contains mass spectra and retention index information of over 1000 authentic chemical standards, which were cross-checked with commercial GC-MS databases such as NIST20 spectral library and Wiley 11th version GC-MS databases. Three unique fragmented ions were selected and used to integrate peak area values, and a few metabolites were curated manually, when necessary.

2.5 | DNA extraction followed by amplicon and metagenomic sequencing

We extracted DNA from the rhizoplane and rhizosphere for each tree species and each root order (R1/2 and R4/5). DNA was extracted using a NucleoSpin 96 Soil DNA extraction kit (Machery-Nagel; catalogue: 740787.2) as per the manufacturer's instructions using 300 μ L of rhizoplane or rhizosphere solution. Extracted DNA from the rhizoplane and rhizosphere were subject to 16S rRNA gene (515F and 806R) (Apprill et al., 2015; Parada et al., 2016) and internal transcribed spacer (ITS) region (ITS1F and 58A2R) (Gardes & Bruns, 1993; Martin & Rygielwicz, 2005) amplicon sequencing for characterization of bacterial and fungal composition. The PCR ingredient mixtures for both reactions were as follows: 12 μ L of Platinum II Hot-Start PCR Master Mix, 1.5 μ L of each primer (10 μ M), 1.5 μ L template DNA and 13.5 μ L molecular grade water for a final PCR volume of 30 μ L. PCR cycling conditions for the bacterial 16S rRNA gene were: 3 min at 94°C, 25 cycles of 45 s at 94°C, 60 s at 50°C and 90 s at 72°C and a final elongation step of 10 min at 72°C. PCR cycling conditions for the fungal ITS region were: 3 min at

94°C, 35 cycles of 20 s at 94°C, 30 s at 45°C and 45 s at 72°C, and a final elongation step of 5 min at 72°C. Blank DNA extraction controls and negative PCR controls were also included and no amplicons were observed. Amplicons were cleaned using Mag-Bind TotalPure NGS magnetic beads (Omega Bio-Tek; catalogue: M1378-01). Cleaned amplicons were indexed with the following PCR ingredients: 12.5 μ L of Platinum II Hot-Start PCR Master Mix, 2.5 μ L of each index (10 μ M) and 2.5 μ L of sterile water for a final volume of 25 μ L, and PCR cycling conditions: 1 min at 98°C, eight cycles of 15 s at 98°C, 30 s at 55°C, and 20 s at 72°C, and a final elongation step of 5 min at 72°C. Indexed amplicons were normalized using the SequalPrep normalization plate kit (ThermoFisher; catalogue: A1051001), pooled, concentrated with a speedvac and purified with a gel extraction using the PureLink quick gel extraction kit (ThermoFisher; catalogue: K210012). The pooled library was sequenced on the Illumina MiSeq sequencing platform (2 \times 250 bp) by the Pennsylvania State University Genomics Core Facility (Huck Institutes for the Life Sciences). Shotgun metagenomic sequencing was performed only on the rhizoplane compartment. Library preparation and sequencing on the Illumina NextSeq. 2000 sequencing platform with P2 flowcells (2 \times 150 bp) was performed by the Pennsylvania State University Genomics Core Facility (Huck Institutes for the Life Sciences).

2.6 | Amplicon and metagenomic sequence analysis

Raw demultiplexed 16S rRNA gene and fungal ITS region data were processed using the Quantitative Insights into Microbial Ecology (QIIME 2 version 2020.11) pipeline (Bolyen et al., 2019). First, paired-ended amplicon sequencing data were trimmed and denoised using DADA2, which also removes chimeric sequences (Callahan et al., 2016). Taxonomy was assigned against the Silva v138 (Quast et al., 2013) or UNITE v8.2 (04.02.2020) database (Kõljalg et al., 2005) at the single nucleotide threshold (ZOTUs; zero-radius OTUs) using the classify-sklearn qiime feature classifier. The data set was further cleaned by removing sequences identified as archaea, chloroplasts or mitochondria (272 ZOTUs removed), and by removing ZOTUs with less than 26 (0.002%) and 20 (0.002%) sequences for the 16S rRNA gene and ITS region datasets, respectively. The cleaned 16S rRNA gene and fungal ITS data were then rarefied at 17865 and 6616 sequences per sample, respectively (Supporting Information: Figure 1).

Paired-end rhizoplane shotgun metagenomic data quality were assessed with FastQC (Andrews, 2015) and MultiQC (Ewels et al., 2016). Quality control, trimming, base correction and the removal of polyG tails were performed using fastp (Chen et al., 2018). Cleaned and trimmed metagenomic data were decontaminated using Kneaddata, which uses bowtie2 (Langmead & Salzberg, 2012), in two steps. First, tandem repeats were removed, and the remaining data were decontaminated against the human genome and human contaminants. Next, host-associated metagenomic data were removed by constructing a bowtie2 database using genomes belonging to *Liriodendron chinense* (PRJNA418360), *Acer yangbiense* (PRJNA524417), *Pinus lambertiana* (PRJNA174450), *Pinus taeda* (PRJNA174450), *Quercus aquifolioides* (PRJNA694730) and *Quercus*

lobata (PRJNA574457). At the time of genome collection (11 February 2022), only one genome/species was available for the *Liriodendron* and *Acer* genera. For the *Pinus* and *Quercus* genera, a number of genomes were available and two genomes per species were selected based on how recently the genome was uploaded to NCBI and the species presence in North America. The human- and host plant-decontaminated data were imported into kbase (Arkin et al., 2018) for further analysis. Metagenomic data were taxonomically assigned using GOTTCHA2 (Freitas et al., 2015), which also calculates relative abundance using the roll-up depth of coverage. For functional analysis, a co-assembly was performed for each root order for each tree species using MEGAHIT (Li et al., 2015) and were functionally annotated using DRAM (Shaffer et al., 2020). Assembly quality was checked using QUAST (Gurevich et al., 2013). Raw data files, both amplicon and shotgun metagenomics, in FASTQ format were deposited in the NCBI sequence read archive under Bioproject number PRJNA875879. Code used for the sequence analysis, as well as the final tables, are available at King (2023) (URL: <https://osf.io/5c6gm/>).

2.7 | Statistical analysis

Statistical comparisons were performed in the R statistical environment (R Core Team, 2012). In total, we used 48 samples for the amplicon sequencing analyses (24 rhizosphere and 24 rhizoplane) and 24 samples each for the shotgun metagenomic (rhizoplane) and metabolomic analyses. Comparisons of bacterial and fungal amplicon sequencing data and shotgun metagenomics data were performed using the Phyloseq package (McMurdie & Holmes, 2013). We chose rarefaction and proportional transformation (i.e., relative abundance) as they account for uneven sequencing depth and have been shown to produce the most accurate representations of community-level patterns (McKnight et al., 2019; Weiss et al., 2017). Principal Coordinates Analysis ordinations with a Bray–Curtis dissimilarity index were used to compare microbial composition between tree species and branching root order. Statistical comparisons of microbial composition were performed with a PERMANOVA (Adonis2) from the vegan package with 999 permutations (Oksanen et al., 2015) using the formula Tree species \times Functional root type + Root compartment, and were adjusted to the false discovery rate when needed to account for Type I errors. We tested homogeneity of dispersion with betadisper from the stats package and when using balanced designs, PERMANOVA is largely not impacted by heterogeneity of dispersion (Anderson & Walsh, 2013). To identify taxa associated to different tree species, an indicator species analysis was performed using multipatt from the indicspecies package (Cáceres & Legendre, 2009). To identify taxa with significantly different relative abundance between root compartments or functional root types, a SIMPER analysis was performed from the vegan package with 999 permutations. To compare microbial functional genes, genes were collapsed into metabolism modules (see Shaffer et al. [2020]), normalized to total counts per co-assembly, and converted into copies per million base pairs (i.e., gene count/total counts \times 1000 000), and statistically compared with a Kruskal–Wallis test from the stats package. We compared genes that were present in at least six of eight co-assemblies and with >2-fold change between root orders.

Root metabolome data were imported into the R statistical environment, transformed with autoscaling using the mdatools package (Kucheryavskiy, 2020), compared using a Principal Components Analysis with the Phyloseq package and a PERMANOVA with the vegan package both with a Euclidean distance. To identify which metabolites were contributing to the metabolome differences between root orders, we compared the metabolites using a DESEQ2 differential abundance analysis (Love et al., 2014). To examine relationships between the root metabolome and microbial taxa, a Constrained Analysis of Principal coordinates (CAP) was used with the 10 most abundant genera (metagenomic data) or classes (amplicon sequencing data) and the 10 most abundant metabolites. We also used a weighted gene co-expression network analysis (WGCNA; Langfelder & Horvath [2008]) to investigate connections between the root metabolome and the sequencing data. For the WGCNA, we first used centred-log ratio transformed amplicon data summarized at the class level and metagenomic data summarized at the genus level for taxa found in at least 12 samples. Second, we used the log-transformed metagenomics functional data that was present in at least four samples (as the data had been co-assembled). WGCNA p values were Bonferroni adjusted to the module number.

3 | RESULTS

3.1 | Bacteria and fungi differ according to tree species

Differences between tree species explained the greatest compositional variance for both bacterial (PERMANOVA; $R^2 = 0.15$; Supporting Information: Table 1) and fungal compositions ($R^2 = 0.18$), and we observed a significant interaction between tree species and functional root type for both bacterial (PERMANOVA; $F_{3,44} = 1$, $R^2 = 0.08$, $p = 0.03$; Supporting Information: Table 1) and fungal compositions ($F_{3,44} = 2$, $R^2 = 0.12$, $p \leq 0.001$). Additionally, we detected differences between root compartments for bacterial composition ($F_{1,47} = 3$, $R^2 = 0.04$, $p = 0.006$) but not for fungal composition (Supporting Information: Table 1). Each tree species associated with different higher taxa (Supporting Information: Table 1 and Supporting Information: Figure 2). Notably, the deciduous tree species associated with the *Nitrospirota* and *Sordariomycetes*. The thin-rooted tree species associated with the *Gemmatimonadota* and *Mortierellomycetes*, and the thick-rooted tree species associated with the *Agaricomycetes* (Supporting Information: Table 2).

3.2 | Bacteria differ between root compartments for absorptive fine roots

To further investigate the fine-scale spatial relationship between root compartment and fine root functional type, we compared rhizoplane and rhizosphere root compartments for absorptive and transportive fine roots individually and corrected the p values for multiple testing (Figure 1). For bacterial composition, we observed a significant

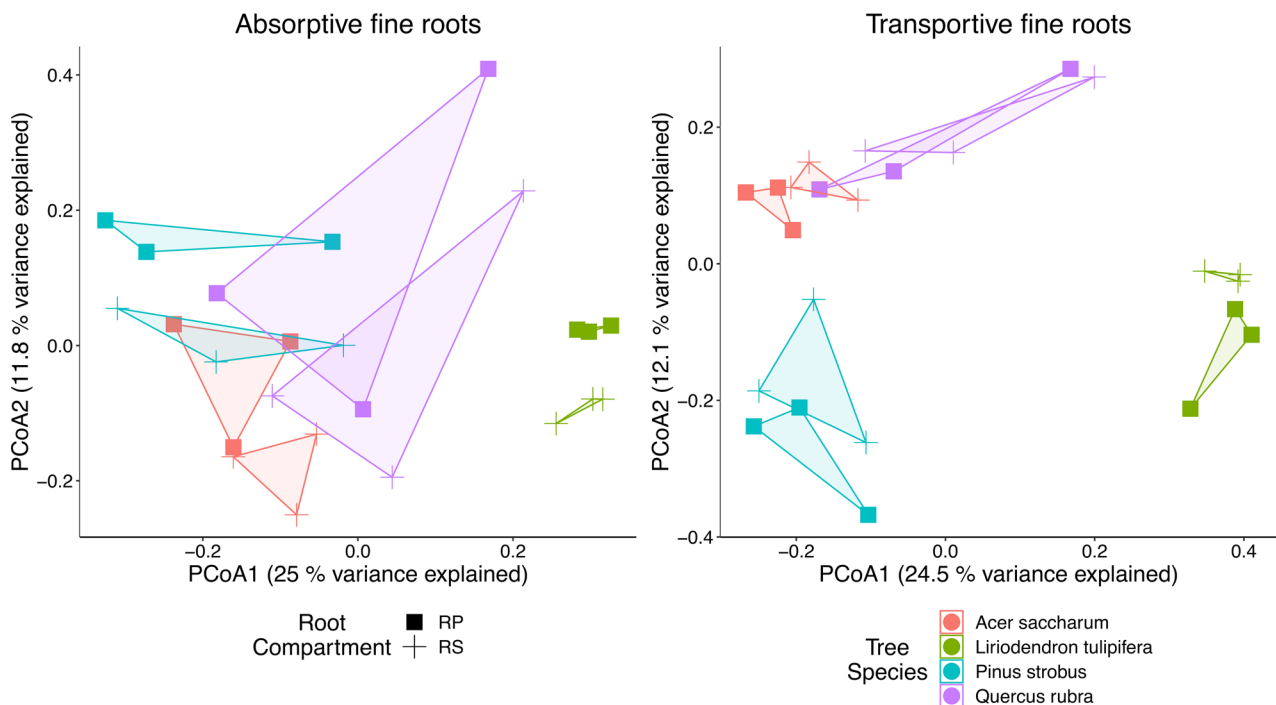


FIGURE 1 Principal Coordinates Analysis (PCoA) ordination of bacterial composition between root compartments for absorptive and transportive fine roots. For the ordination, squares and crosses are the rhizoplane (RP) and rhizosphere (RS) compartments, respectively, and each tree species is a unique colour. We observed a significant difference between root compartments for absorptive fine roots ($q = 0.03$) but not transportive fine roots (PERMANOVA).

difference between the rhizoplane and rhizosphere compartments for absorptive fine roots (PERMANOVA; $F_{1,22} = 2$, $R^2 = 0.07$, $q = 0.03$; Supporting Information: Figure 2) but not transportive fine roots. No differences between root compartments were observed for fungal composition for either functional root type (Supporting Information: Figure 3). We also observed differences among tree species for both absorptive and transportive fine roots (Bacteria R1/2: $F_{3,20} = 4$, $R^2 = 0.36$, $q \leq 0.001$; Bacteria R4/5: $F_{3,20} = 4$, $R^2 = 0.40$, $q \leq 0.001$; Fungi R1/2: $F_{3,20} = 3$, $R^2 = 0.35$, $q \leq 0.001$; Fungi R4/5: $F_{3,20} = 4$, $R^2 = 0.40$, $q \leq 0.001$; Supporting Information: Figure 2). The absorptive fine root rhizoplane had a significantly greater average relative abundance of the *Alphaproteobacteria* (SIMPER; $p \leq 0.001$) and *Gammaproteobacteria* ($p = 0.004$) classes, while the absorptive fine root rhizosphere had a greater average relative abundance of the *Verrucomicrobiae* ($p = 0.05$) and the *Vicinamibacteria* ($p = 0.002$) classes (Supporting Information: Figure 4).

3.3 | Rhizoplane bacterial composition and function differ according to root functional type

We previously identified that the ectorhizosphere (combined rhizosphere and rhizoplane) significantly differed between absorptive and transportive fine roots, but it was unclear whether the rhizosphere or rhizoplane primarily contributed to the microbial differences. Here, we compared microbial composition between absorptive and

transportive fine roots for individual root compartments to identify whether root functional type differentially impacts bacterial and fungal composition (Figure 2). For bacterial composition, we observed a significant difference between the absorptive and transportive fine roots for rhizoplane bacteria (PERMANOVA; $F_{1,22} = 2$, $R^2 = 0.05$, $q = 0.04$) but failed to find differences for rhizosphere bacteria. No differences between functional root types were observed for fungal composition when comparing individual root compartments (Supporting Information: Figure 5). Differences between tree species were also observed for both rhizoplane (Bacteria: $F_{3,20} = 4$, $R^2 = 0.33$, $q \leq 0.001$; Fungi: $F_{3,20} = 3$, $R^2 = 0.32$, $q \leq 0.001$) and rhizosphere (Bacteria: $F_{3,20} = 4$, $R^2 = 0.37$, $q \leq 0.001$; Fungi: $F_{3,20} = 4$, $R^2 = 0.38$, $q \leq 0.001$) microorganisms. The absorptive fine root rhizoplane had a significantly greater average relative abundance of the *Gammaproteobacteria* (SIMPER; $p = 0.003$; Supporting Information: Figure 4; primarily composed of the class *Burkholderiales* (61%), formerly the *Betaproteobacteria*) and *Bacteroidia* ($p = 0.01$) classes, while the transportive fine root rhizoplane had a greater average relative abundance of the *TK10* ($p = 0.05$) and the *Abditibacteria* ($p = 0.001$) classes (Supporting Information: Figure 4). Analyses of rhizoplane shotgun metagenomic data additionally confirmed that tree species explain the greatest compositional variance (PERMANOVA; $R^2 = 0.40$), and the significant interaction between tree species and functional root type (PERMANOVA; $F_{3,20} = 2$, $R^2 = 0.13$, $p = 0.03$; Supporting Information: Figure 6). Species assigned to the *Bradyrhizobium* and *Rhizobium* genera were consistently the most relatively

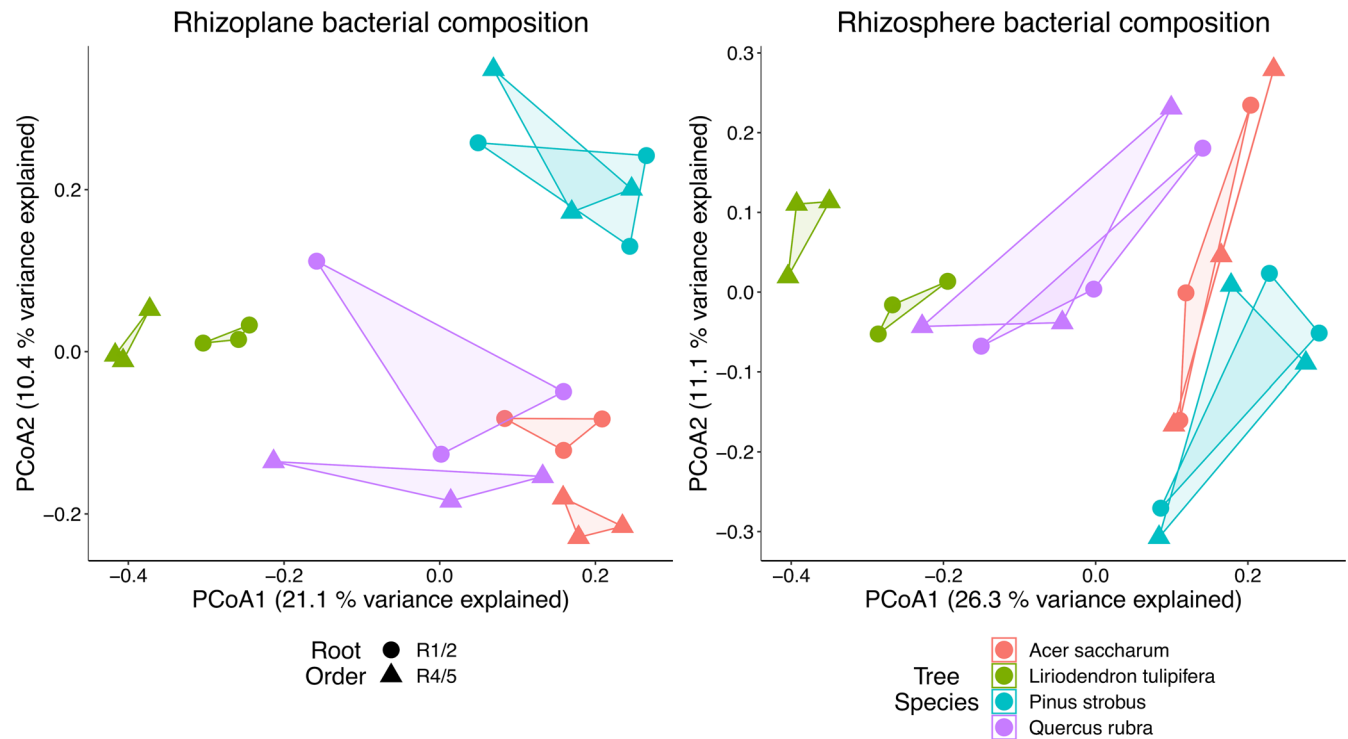


FIGURE 2 Principal Coordinates Analysis (PCoA) ordination of rhizoplane and rhizosphere bacterial composition between root functional types. For the ordination, circles and triangles are the absorptive (i.e., R1/2) and transportive (i.e., R4/5) fine roots, respectively, and each tree species is a unique colour. We observed a significant difference between root functional types for rhizoplane bacteria ($q = 0.04$) but not for rhizosphere bacteria (PERMANOVA). [Color figure can be viewed at [wileyonlinelibrary.com](https://onlinelibrary.wiley.com)]

abundant in the rhizoplane (Supporting Information: Table 3). Functions assigned to a number of sugar transport systems, isopeptidases and endopeptidases were overrepresented in microbes associated with absorptive fine roots, while dipeptidases and the urea transport system were more abundant in microbes associated with transportive fine roots (Supporting Information: Table 4).

3.4 | Root metabolomes differ by root functional type

We performed a metabolomic analysis to identify whether the resources available from absorptive and transportive fine roots could help explain microbial assembly patterns (Figure 3). Root metabolomes differed significantly according to root functional type (PERMANOVA; $F_{1,22} = 2$, $R^2 = 0.09$, $p = 0.03$) but not tree species. Across the data set, sucrose was the most highly abundant metabolite identified (13% average relative abundance) followed by quinic acid (13%). Between the root functional types, the metabolites with the greatest significant fold increase in relative abundance in the absorptive fine roots were D-sorbitol (DESEQ2 differential abundance; 20.8-fold; Supporting Information: Table 5), nicotinic acid (15-fold), trehalose (14.7-fold), and D-mannitol (9-fold), while L-ornithine (28-fold), chiro-inositol (9-fold), and 3-amino-2-piperidone (8-fold) had the greatest significant fold increase in the transportive fine

roots. Additionally, a number of amino acids were enriched in the absorptive fine roots including isoleucine, cysteine and valine, and fatty acids including oleic acid and palmitic acid (Supporting Information: Table 5).

We sought to examine relationships between bacterial taxa and the root metabolome by fitting the most abundant metabolites against the shotgun metagenomic and amplicon sequencing data (Figure 4). Both the metagenomic (ANOVA; $F_{10,13} = 3$, adjusted- $R^2 = 0.54$, $p \leq 0.001$) and amplicon (bacteria: $F_{10,13} = 2$, adjusted- $R^2 = 0.45$, $p = 0.002$; Fungi: $F_{10,13} = 2$, adjusted- $R^2 = 0.40$, $p = 0.01$) ordinations were a significant representation of the data. On the first CAP axis, increasing sucrose, unknown compound 90, catechin and epicatechin were observed with decreasing phosphate ion and malic acid. On the second CAP axis, trehalose abundance was negatively associated with quinic acid, tagatose and D-fructose. The *Rhizobium* and *Paraburkholderia* genera and *Gammaproteobacteria* and *Dothideomycetes* classes increased with increasing trehalose. The *Stenotrophomonas* genus and *Alphaproteobacteria* class increased with increasing D-fructose and tagatose, as did the *Mortierellomycetes*, an unclassified *Rozellomycotina* and the *Leotiomyces* classes. The *Bradyrhizobium* genus, and the *Acidobacteriae*, *Verrucomicrobiae* and *Sordariomycetes* classes were associated with sucrose.

We used a WGCNA to identify correlations across data sets. First, we compared the sequencing data (amplicon and shotgun metagenomic) to the root metabolome data (Figure 4 and Supporting

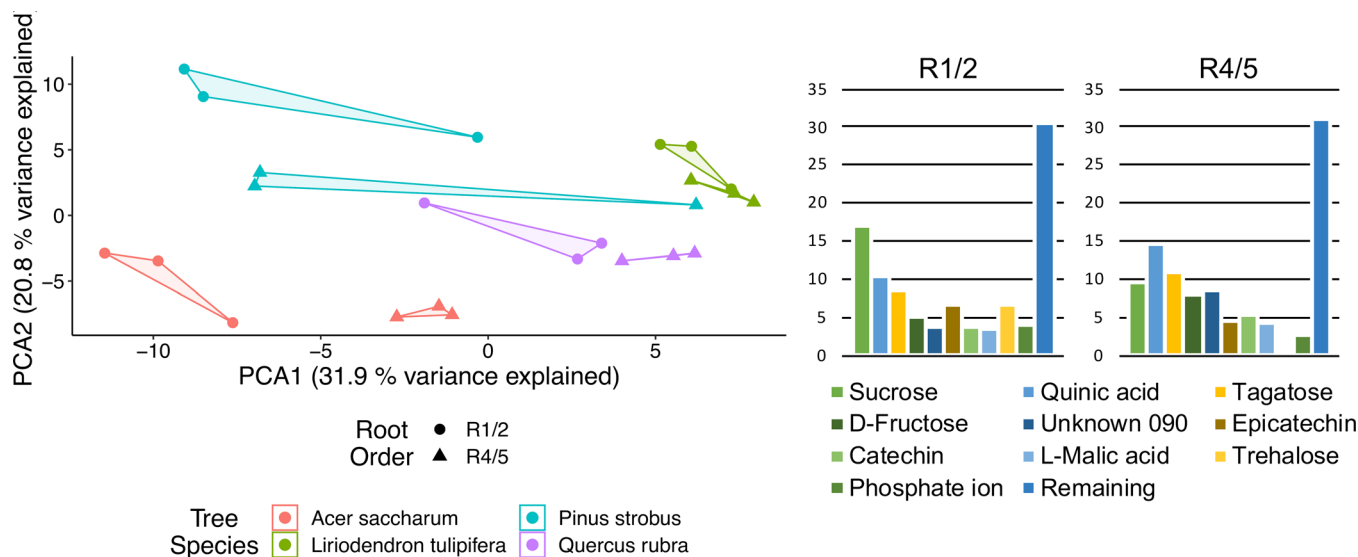


FIGURE 3 Principal Components Analysis (PCA) ordination of root metabolomes for absorptive and transportive fine roots and metabolome composition. For the ordination, circles and triangles are the absorptive (i.e., R1/2) and transportive (i.e., R4/5) fine roots, respectively, and each tree species is a unique colour. The average relative abundance (%) of root metabolites for the absorptive and transportive fine roots are shown. The root metabolome was significantly different between root functional types ($p = 0.03$; PERMANOVA). [Color figure can be viewed at [wileyonlinelibrary.com](https://onlinelibrary.wiley.com/doi/10.1111/pce.14705)]

Information: Table 5; Supporting Information: File 2). Metabolites that were primarily significantly overrepresented in the absorptive fine roots were assigned to modules blue and turquoise, while metabolites that were primarily overrepresented in the transportive fine roots were assigned to modules grey and yellow (Supporting Information: File 2 and Supporting Information: Table 5). We observed the most correlations with bacterial taxa with the turquoise module, which included positive correlations with sequences assigned to the *Actinobacteria*, *Rubrobacteria* and *Chloroflexia* classes, and negative correlations with the *Rhodoplanes* genus and the *Verrucomicrobiae* class. The blue module included negative correlations with the relative abundance of taxa in the rhizosphere and the *Solirubrobacter* genus. For the grey and yellow modules, we only observed negative correlations with a number of classes assigned to the phylum *Acidobacteriota* (subgroup 11 and 5, and the *Holophagae*) and the predatory *Oligoflexia* and *bacteriap25* (Myxococota) classes.

Correlations between the metagenomic functional data and the metabolome were primarily driven by peptidases (Supporting Information: Table 6). For this separate analysis, most absorptive fine root metabolites (Supporting Information: Table 5) were assigned to the blue and grey modules, and the grey module was associated with unassigned peptidases, while transportive fine root metabolites were primarily assigned to the brown module (Supporting Information: File 2) and associated with membrane-bound bacterial endopeptidases.

4 | DISCUSSION

Fine root classification has implications for various ecological processes, including fine-scale biogeochemical cycling and root-microbial relationships. Functionally discrete fine roots have been

shown to differ by a number of metrics, including respiratory activity, morphology, nutrient concentration, root hair density and absorptive capacity (Fan & Guo, 2010; Gordon & Jackson, 2000; Hishi, 2007; McCormack et al., 2015; Minerovic et al., 2018; Pregitzer et al., 2002; Segal et al., 2008; Valenzuela-Estrada et al., 2008). We would expect that, due to differences in how these roots influence the surrounding environment, microbial assembly should follow similar trends. In this study, we investigated how fine root functional type (determined by branching root order) from four diverse tree species that varied widely in root morphology and mycorrhizal association impacts microbial composition in two root compartments and whether the resources available for each root functional type also differed. Overall, we identified a significant interaction between tree species and root functional type for both bacterial and fungal composition. Bacterial compositions were found to be distinct between root microbiome compartments for absorptive fine roots. Root functional type was a significant driver of the bacterial rhizoplane, but not rhizosphere, composition, and the resources available in absorptive and transportive fine roots (i.e., the root metabolome) also differed (Figure 5).

Plants shape their root microbiome through a number of processes, including carbon exudation and modifications to habitat space, but the degree of selective pressure is different for different root compartments. For rice, there is a gradient of host-driven microbiome filtering, with the host influence being lowest in the rhizosphere, followed by the rhizoplane, and endosphere (root interior) (Edwards et al., 2015). Similar filtering patterns with decreasing host influence with further distance to the root surface have been observed for other plants (Lang et al., 2019; Tkacz et al., 2020; Zhong et al., 2022). However, these studies either homogenized roots or did not clearly state that roots were sorted

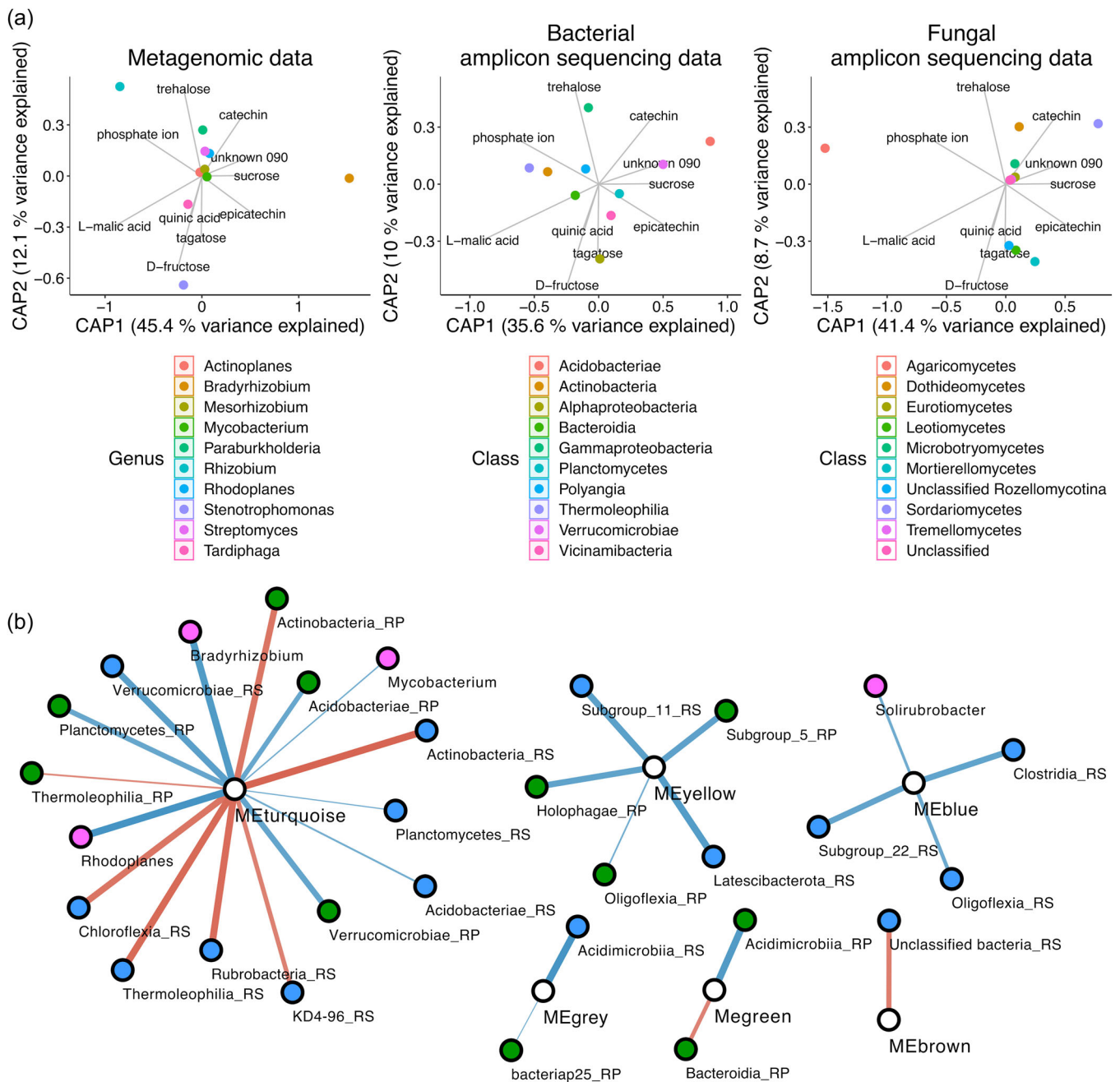


FIGURE 4 Relationships between microbial data and root metabolome data. (a) Ordinations of bacterial and fungal composition with root metabolome data. Each ordination is a constrained analysis of principal coordinates (CAP). Metagenomic data were summarized at the genus level, while amplicon sequencing data were summarized at the class level. The root metabolome was fitted as environmental variables. The top 10 most abundant metabolites and the top 10 most abundant taxa were used. (b) Visualization of a weighted gene co-expression network analysis. Shown data are Bonferroni-corrected significant interaction and Pearson's correlations. Red lines (edges) are positive correlations. The edge line thickness is the size of the q-value, with smaller q-values yielding thicker edges. Data include the bacterial and fungal amplicon sequencing data summarized at the Class level, and metagenomic data (pink nodes) summarized at the Genus level. Correlations were performed for rhizoplane (RP; green nodes) and rhizosphere (RS; blue nodes) taxa. Taxa are correlated to modules of metabolites, which are viewable as Supporting Information: File 2. [Color figure can be viewed at [wileyonlinelibrary.com](https://onlinelibrary.wiley.com)]

before microbial analyses, so it is unclear whether host-driven filtering is consistent across fine root functional types. In our study, rhizoplane and rhizosphere bacterial composition were significantly different for absorptive, but not transportive fine roots. The contrasting bacterial patterns between absorptive and transportive

fine roots can likely be explained by host physiology. Absorptive fine roots are expected to exert stronger selection pressure on their local environment through increased rhizodeposition and greater nutrient and water influx relative to transportive fine roots (McCormack et al., 2015), which is also a gradient of influence (Kuzyakov &

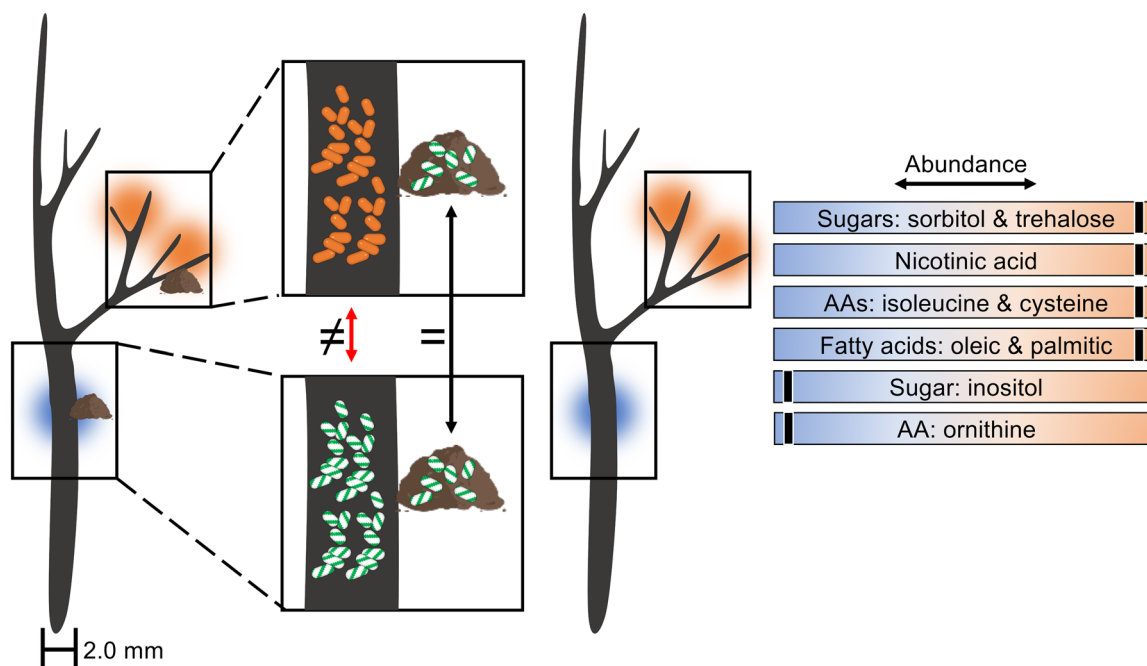


FIGURE 5 Conceptual figure of the bacterial rhizoplane, bacterial rhizosphere and the root metabolome. Rhizoplane bacteria were significantly different between absorptive (orange cells) and transportive (green cells) fine roots (indicated by \neq), while rhizosphere bacteria were not significantly different (indicated by $=$). Rhizoplane bacteria on the absorptive fine roots (orange cells) were different from the rhizosphere bacteria (green cells), but no differences were observed between root compartments on the transportive fine roots (both green cells). The root metabolome was different according to root functional type, with large shifts in sugars, amino acids (AAs), and fatty acids. A not to scale size key is provided to highlight that traditional size exclusion approaches (i.e., all roots <2 mm) would homogenize the displayed root cluster. [Color figure can be viewed at wileyonlinelibrary.com]

Razavi, 2019). Possibly, the root-associated gradient of influence for transportive fine roots is minimal resulting in similar microbial composition between root compartments.

In this study, we observed a curious pattern where rhizoplane bacteria were distinct between absorptive and transportive fine roots, but rhizosphere bacteria were not. The bacterial rhizoplane differences between absorptive and transportive fine roots could be explained by resource availability as we also detected differences with the root metabolome data and with potential microbial functions (i.e., sugar transport, peptidases and urea transport). The similarity of the rhizosphere bacteria between absorptive and transportive fine roots was surprising as we would expect host rhizodeposition to be greater by the absorptive fine roots and, therefore, to have an influence in shaping the composition of the rhizosphere bacteria. It is well known that the plant rhizosphere is distinct from the surrounding bulk soil (Edwards et al., 2015; Lang et al., 2019; Tkacz et al., 2020; Zhong et al., 2022), and it is generally assumed that the resources released by the roots play a strong role shaping that rhizosphere. It could be that the host-released resources that survive rhizoplane consumption are comparable for the absorptive and transportive fine roots, or the rhizosphere soil could be co-influenced by multiple root segments.

Resource abundance and diversity can be important factors influencing microbial diversity and composition (Bell et al., 2021;

Langenheder & Prosser, 2008; She et al., 2018). We detected differences between absorptive and transportive fine roots for the root metabolome, which were primarily linked to a greater relative abundance of the sugars sorbitol, trehalose and mannitol in the absorptive fine roots and inositol in the transportive fine roots, amino acids isoleucine, cysteine and valine in the absorptive fine roots, and ornithine and asparagine in the transportive fine roots, and the fatty acids oleic acid and palmitic acid in the absorptive fine roots.

A correlation network analysis with microbial taxa grouped the majority of the absorptive fine root metabolites into the blue module followed by the turquoise module (Figure 4 and Supporting Information: File 2). In either case, we observed more correlations with the relative abundance of rhizosphere taxa relative to rhizoplane taxa. As a general pattern, particularly for the turquoise model, classes assigned to the *Actinomyetota* phylum drove many of the positive correlations, including the *Actinobacteria*, *Rubrobacteria* and *Thermoleophilia* classes. In support of our data, the *Actinomyetota* are typically enriched in the root microbiome/rhizosphere (Ling et al., 2022) and many are strong competitors due to the production of certain secondary metabolites (Barka et al., 2015). We also observed a higher relative abundance of the *Gammaproteobacteria* class (primarily composed of the formally named *Betaproteobacteria* class) in the absorptive fine root rhizoplane, which corresponded with trehalose abundance. In agreement with our data, the *Betaproteobacteria* have been implicated for their role in

carbon mineralization (Fierer et al., 2007) and we previously observed greater relative abundances of the *Betaproteobacteria* in absorptive fine roots (King et al., 2021), reinforcing that copiotrophic bacteria may preferentially colonize absorptive fine roots. On the other hand, transportive fine root metabolites were assigned to the grey and yellow modules and we observed negative correlations with an unclassified class in the *Latescibacterota* phylum and two predatory bacterial classes (*Oligoflexia* and *bacteriap25* [*Myxococcota*]). In some environments, bacteria assigned to the *Latescibacterota* and *Myxococcota* phyla have been observed to have a high degree of carbohydrate-active enzyme diversity (Martínez-Pérez et al., 2022). In our study, the *Latescibacterota* and *Oligoflexia* were negatively correlated with the yellow module which had one of the lowest numbers of assigned metabolites. We also expect the microbial carrying capacity to be greater on the absorptive fine roots (King et al., 2021), particularly with the greater abundances of certain sugars we observed in this study, which may impact the relative abundances of predatory bacteria (e.g., the *Oligoflexia* class in the *Bdellovibrionota*) and explain the negative correlations of these taxa with the transportive fine root metabolites.

For the transportive fine roots, we observed a greater relative abundance of the nonproteinogenic amino acid ornithine and an enrichment of a microbial function assigned to the urea transport system. Ornithine has important implications for arginine cycling. Arginine is an important nitrogen storage molecule as it has the lowest carbon-to-nitrogen ratio of the proteinogenic amino acids, and is one of the major forms of nitrogen storage in roots (Nordin & Näsholm, 1997). Ornithine can be used to synthesize arginine or arginine can be catabolized to ornithine and urea (Winter et al., 2015), which corresponds to the overrepresentation of ornithine and urea transport in the transportive fine roots in our study. Transportive fine roots could be important for nitrogen storage and transport, and the leakage of these molecules may impact microbial composition and function on the rhizoplane.

For both bacteria and fungi, we identified differences among tree species and a significant interaction between tree species and root functional type. Similar to bacteria, fungal compositional differences between root functional types are likely driven by differences in fine root physiology and morphology (McCormack et al., 2015). However, when comparing individual compartments or individual root functional types, differences were primarily based on bacterial composition. Further, we identified differences between root compartments for bacteria but not fungi. A recent study using unsorted roots examined the influence of root compartment, soil type (two soils) and plant species (four herbaceous plants) on bacterial and fungal composition (Tkacz et al., 2020). Root compartment was the strongest driver of bacterial composition, but soil type was a stronger driver of fungal composition (Tkacz et al., 2020). Soils across our common garden were relatively homogeneous at the time of planting, which may help explain the fungal similarity between root compartments. Fungal hyphae may also extend from the rhizoplane root compartment toward the rhizosphere obscuring fungal composition differences between root compartments. The lack of significance for further spatial comparisons for fungi may also be due to sample size. We know sample size is a limitation of this study; however, we can conclude that fungi are assembled according to root functional type and further

studies can elaborate on the spatial patterns driving fine-scale fungal assembly with additional tree species.

Differences between tree species explained the greatest compositional variance for bacterial and fungal composition. Trees may structure their surrounding soil through rhizodeposition and litter quality, which are often driven by mycorrhizal association, thereby altering the abiotic conditions of their local environment (Jiang et al., 2023; Kuzyakov & Razavi, 2019; Midgley et al., 2015; Yates et al., 2021). A previous study at our study site examined tree-mediated differences in soil chemical properties (Yates et al., 2021). Soils associated with *P. strobus* were found to have the lowest pH and available nitrogen. In our data, an indicator species analysis identified the *Nitrospirota* phylum as being significantly associated with the three deciduous tree species, and not the conifer *P. strobus*. In agreement with our observation, nitrification is susceptible to decreasing pH (Sharma & Ahlert, 1977) which could impact *Nitrospirota* relative abundance. Despite the relatively stronger influence of tree species on microbial assemblage, we detected differences between root functional type and root microbiome compartments and these differences should be considered when examining microbial composition.

Deciphering host-microbial relationships requires an intricate understanding of the host physiology and morphology. Studies of root microbiomes have largely involved root homogenization, which does not acknowledge the substantial heterogeneity of root morphology and physiology between root functional types. Here, we have shown that different root compartments are differentially structured by root functional type and the resources available at functionally discrete fine roots also being distinct. Bacteria and fungi were both significantly influenced by root functional type, but bacteria were further spatially structured with differences detected according to root functional type for the rhizoplane and between root compartments for the absorptive fine roots. Distinct bacterial assembly patterns were confirmed with both amplicon sequencing and shotgun metagenomic data, and we observed differences in microbial functional potential associated with sugar transport, peptidases and urea transport. Metabolomic data revealed differences in the resources available at each root functional type, which was primarily driven by the differential abundance of sugars, amino acids and fatty acids. Classes assigned to the *Actinomycetota* phylum were correlated to a number of absorptive fine root metabolites, and the *Betaproteobacteria* (within the *Gammaproteobacteria* class) were associated with disaccharide sugars and had a greater relative abundance on absorptive fine roots which may be related to their presumed copiotrophic lifestyle (Fierer et al., 2007). Overall, our data provide further evidence that microbial composition is spatially structured according to root functional type and that there are differing selective pressures for each root compartment for different root functional types. These data highlight the need to consider root physiology when examining root-microbial feedback and the potential to dampen subtle microbial signals.

ACKNOWLEDGEMENTS

This research was supported by the USDA National Institute of Food and Agriculture (NIFA) Federal Appropriation under Project #PEN0

4628 (Accession #1014131), Project #PEN0 4744 (Accession #1023222) and Project #PEN0 4651 (Accession #1016233). Analysis and writing were partly supported by USDA ORG Project PENW-2019-03513 and the National Science Foundation (NSF) Centre for Research on Programmable Plant Systems (CROPPS; Grant number #DBI-2019674). A portion of this research was performed on a project award (doi.org/10.46936/ltids.proj.2021.60134/60000418 awarded to WLK, THB and DME) from the Environmental Molecular Sciences Laboratory, a DOE Office of Science User Facility sponsored by the Biological and Environmental Research program under Contract No. DE-AC05-76RLO 1830. Pacific Northwest National Laboratory is a multiprogram national laboratory operated by Battelle for the US DOE under contract DE-AC05-76RLO 1830.

CONFLICT OF INTEREST STATEMENT

The authors declare no conflict of interest.

DATA AVAILABILITY STATEMENT

Raw data files in FASTQ format were deposited in the NCBI sequence read archive under Bioproject number PRJNA875879.

ORCID

William L. King  <http://orcid.org/0000-0001-7272-8242>

Benjamin D. Hafner  <https://orcid.org/0000-0003-2348-9200>

Christopher R. Anderton  <https://orcid.org/0000-0002-6170-1033>

Terrence H. Bell  <https://orcid.org/0000-0003-3603-7270>

REFERENCES

- Anderson, M.J. & Walsh, D.C.I. (2013) PERMANOVA, ANOSIM, and the mantel test in the face of heterogeneous dispersions: what null hypothesis are you testing? *Ecological Monographs*, 83(4), 557–574.
- Andrews, S. (2015) FastQC: A Quality Control Tool for High Throughput Sequence Data[Online].
- Apprill, A., McNally, S., Parsons, R. & Weber, L. (2015) Minor revision to V4 region SSU rRNA 806R gene primer greatly increases detection of SAR11 bacterioplankton. *Aquatic Microbial Ecology*, 75, 129–137.
- Arkin, A.P., Cottingham, R.W., Henry, C.S., Harris, N.L., Stevens, R.L., Maslov, S. et al. (2018) KBase: the United States department of energy systems biology knowledgebase. *Nature Biotechnology*, 36(7), 566–569.
- Barka, E.A., Vatsa, P., Sanchez, L., Gaveau-Vaillant, N., Jacquard, C., Klenk, H.-P. et al. (2015) Taxonomy, physiology, and natural products of actinobacteria. *Microbiology and Molecular Biology Reviews*, 80(1), 1–43.
- Bell, T.H., Camillone, N., Abram, K., Bruns, M.A., Yergeau, E. & St-Arnaud, M. (2021) Hydrocarbon substrate richness impacts microbial abundance, microbiome composition, and hydrocarbon loss. *Applied Soil Ecology*, 165, 104015.
- Bolyen, E., Rideout, J.R., Dillon, M.R., Bokulich, N.A., Abnet, C.C., Al-Ghalith, G.A. et al. (2019) Reproducible, interactive, scalable and extensible microbiome data science using QIIME 2. *Nature Biotechnology*, 37(8), 852–857.
- Bulgarelli, D., Rott, M., Schlaeppi, K., Ver Loren van Themaat, E., Ahmadinejad, N., Assenza, F. et al. (2012) Revealing structure and assembly cues for *Arabidopsis* root-inhabiting bacterial microbiota. *Nature*, 488(7409), 91–95.
- Bulgarelli, D., Schlaeppi, K., Spaepen, S., van Themaat, E.V.L. & Schulze-Lefert, P. (2013) Structure and functions of the bacterial microbiota of plants. *Annual Review of Plant Biology*, 64(1), 807–838.
- Cáceres, M.D. & Legendre, P. (2009) Associations between species and groups of sites: indices and statistical inference. *Ecology*, 90(12), 3566–3574.
- Callahan, B.J., McMurdie, P.J., Rosen, M.J., Han, A.W., Johnson, A.J.A. & Holmes, S.P. (2016) DADA2: high-resolution sample inference from illumina amplicon data. *Nature Methods*, 13(7), 581–583.
- Chen, L., Brookes, P.C., Xu, J., Zhang, J., Zhang, C., Zhou, X. et al. (2016) Structural and functional differentiation of the root-associated bacterial microbiomes of perennial ryegrass. *Soil Biology and Biochemistry*, 98, 1–10.
- Chen, S., Zhou, Y., Chen, Y. & Gu, J. (2018) fastp: an ultra-fast all-in-one FASTQ preprocessor. *Bioinformatics*, 34(17), i884–i890.
- Edwards, J., Johnson, C., Santos-Medellín, C., Lurie, E., Podishetty, N.K. & Bhatnagar, S. et al. (2015) Structure, variation, and assembly of the root-associated microbiomes of rice. *Proceedings of the National Academy of Sciences*, 112(8), E911.
- Ewels, P., Magnusson, M., Lundin, S. & Käller, M. (2016) MultiQC: summarize analysis results for multiple tools and samples in a single report. *Bioinformatics*, 32(19), 3047–3048.
- Fan, P. & Guo, D. (2010) Slow decomposition of lower order roots: a key mechanism of root carbon and nutrient retention in the soil. *Oecologia*, 163(2), 509–515.
- Fierer, N., Bradford, M.A. & Jackson, R.B. (2007) Toward an ecological classification of soil bacteria. *Ecology*, 88(6), 1354–1364.
- Fitter, A.H. (1982) Morphometric analysis of root systems: application of the technique and influence of soil fertility on root system development in two herbaceous species. *Plant, Cell & Environment*, 5(4), 313–322.
- Fitzpatrick, C.R., Copeland, J., Wang, P.W., Guttman, D.S., Kotanen, P.M. & Johnson, M.T.J. (2018) Assembly and ecological function of the root microbiome across angiosperm plant species. *Proceedings of the National Academy of Sciences*, 115(6), E1157.
- Fleishman, S.M., Eissenstat, D.M., Bell, T.H. & Centinari, M. (2022) Functionally-explicit sampling can answer key questions about the specificity of plant–microbe interactions. *Environmental Microbiome*, 17, 51.
- Freitas, T.A.K., Li, P.-E., Scholz, M.B. & Chain, P.S.G. (2015) Accurate read-based metagenome characterization using a hierarchical suite of unique signatures. *Nucleic Acids Research*, 43(10), e69–e69.
- Gardes, M. & Bruns, T.D. (1993) ITS primers with enhanced specificity for basidiomycetes—application to the identification of mycorrhizae and rusts. *Molecular Ecology*, 2(2), 113–118.
- Gordon, W.S. & Jackson, R.B. (2000) Nutrient concentrations in fine roots. *Ecology*, 81(1), 275–280.
- Gu, J., Yu, S., Sun, Y., Wang, Z. & Guo, D. (2011) Influence of root structure on root survivorship: an analysis of 18 tree species using a minirhizotron method. *Ecological Research*, 26(4), 755–762.
- Guo, D., Mitchell, R.J., Withington, J.M., Fan, P.-P. & Hendricks, J.J. (2008) Endogenous and exogenous controls of root life span, mortality and nitrogen flux in a longleaf pine forest: root branch order predominates. *Journal of Ecology*, 96(4), 737–745.
- Guo, D., Xia, M., Wei, X., Chang, W., Liu, Y. & Wang, Z. (2008) Anatomical traits associated with absorption and mycorrhizal colonization are linked to root branch order in twenty-three Chinese temperate tree species. *New Phytologist*, 180(3), 673–683.
- Gurevich, A., Saveliev, V., Vyahhi, N. & Tesler, G. (2013) QUASt: quality assessment tool for genome assemblies. *Bioinformatics*, 29(8), 1072–1075.
- Hiller, K., Hangebrauk, J., Jäger, C., Spura, J., Schreiber, K. & Schomburg, D. (2009) MetaboliteDetector: comprehensive analysis tool for targeted and nontargeted GC/MS based metabolome analysis. *Analytical Chemistry*, 81(9), 3429–3439.
- Hishi, T. (2007) Heterogeneity of individual roots within the fine root architecture: causal links between physiological and ecosystem functions. *Journal of Forest Research*, 12(2), 126–133.

- Holdaway, R.J., Richardson, S.J., Dickie, I.A., Peltzer, D.A. & Coomes, D.A. (2011) Species- and community-level patterns in fine root traits along a 120 000-year soil chronosequence in temperate rain forest. *Journal of Ecology*, 99(4), 954–963.
- Hu, L., Robert, C.A.M., Cadot, S., Zhang, X., Ye, M., Li, B. et al. (2018) Root exudate metabolites drive plant-soil feedbacks on growth and defense by shaping the rhizosphere microbiota. *Nature Communications*, 9(1), 2738.
- Jiang, O., Li, L., Duan, G., Gustave, W., Zhai, W., Zou, L. et al. (2023) Root exudates increased arsenic mobility and altered microbial community in paddy soils. *Journal of Environmental Sciences*, 127, 410–420.
- Kim, Y.-M., Nowack, S., Olsen, M.T., Becraft, E.D., Wood, J.M., Thiel, V. et al. (2015) Diel metabolomics analysis of a hot spring chlorophototrophic microbial mat leads to new hypotheses of community member metabolisms. *Frontiers in Microbiology*, 6, 209.
- Kind, T., Wohlgemuth, G., Lee, D.Y., Lu, Y., Palazoglu, M., Shahbaz, S. et al. (2009) FiehnLib: mass spectral and retention index libraries for metabolomics based on quadrupole and time-of-flight gas chromatography/mass spectrometry. *Analytical Chemistry*, 81(24), 10038–10048.
- King, W.L. (2023) Functionally discrete fine roots differ in microbial assembly, microbial functional potential, and produced metabolites—code and sequence analysis. *Open Science Framework*. <https://doi.org/10.17605/OSF.IO/5C6GM>
- King, W.L., Yates, C.F., Guo, J., Fleishman, S.M., Trexler, R.V., Centinari, M. et al. (2021) The hierarchy of root branching order determines bacterial composition, microbial carrying capacity and microbial filtering. *Communications Biology*, 4(1), 483.
- Köljal, U., Larsson, K.-H., Abarenkov, K., Nilsson, R.H., Alexander, I.J., Eberhardt, U. et al. (2005) UNITE: a database providing web-based methods for the molecular identification of ectomycorrhizal fungi. *New Phytologist*, 166(3), 1063–1068.
- Kucheryavskiy, S. (2020) mdatools—R package for chemometrics. *Chemometrics and Intelligent Laboratory Systems*, 198, 103937.
- Kuzyakov, Y. & Razavi, B.S. (2019) Rhizosphere size and shape: temporal dynamics and spatial stationarity. *Soil Biology and Biochemistry*, 135, 343–360.
- Lang, M., Bei, S., Li, X., Kuyper, T.W. & Zhang, J. (2019) Rhizoplane bacteria and plant species co-determine phosphorus-mediated microbial legacy effect. *Frontiers in Microbiology*, 10, 2856.
- Langenheder, S. & Prosser, J.I. (2008) Resource availability influences the diversity of a functional group of heterotrophic soil bacteria. *Environmental Microbiology*, 10(9), 2245–2256.
- Langfelder, P. & Horvath, S. (2008) WGCNA: an R package for weighted correlation network analysis. *BMC Bioinformatics*, 9(1), 559.
- Langmead, B. & Salzberg, S.L. (2012) Fast gapped-read alignment with Bowtie 2. *Nature Methods*, 9(4), 357–359.
- Li, D., Liu, C.M., Luo, R., Sadakane, K. & Lam, T.W. (2015) MEGAHIT: an ultra-fast single-node solution for large and complex metagenomics assembly via succinct de Bruijn graph. *Bioinformatics*, 31(10), 1674–1676.
- Ling, N., Wang, T. & Kuzyakov, Y. (2022) Rhizosphere bacteriome structure and functions. *Nature Communications*, 13(1), 836.
- Love, M.I., Huber, W. & Anders, S. (2014) Moderated estimation of fold change and dispersion for RNA-seq data with DESeq. 2. *Genome Biology*, 15(12), 550.
- Luke McCormack, M., Adams, T.S., Smithwick, E.A.H. & Eissenstat, D.M. (2012) Predicting fine root lifespan from plant functional traits in temperate trees. *New Phytologist*, 195(4), 823–831.
- Lundberg, D.S., Lebeis, S.L., Paredes, S.H., Yourstone, S., Gehring, J., Malfatti, S. et al. (2012) Defining the core *Arabidopsis thaliana* root microbiome. *Nature*, 488(7409), 86–90.
- Makita, N., Hirano, Y., Dannoura, M., Kominami, Y., Mizoguchi, T., Ishii, H. et al. (2009) Fine root morphological traits determine variation in root respiration of *Quercus serrata*. *Tree Physiology*, 29(4), 579–585.
- Martin, K.J. & Rygielwicz, P.T. (2005) Fungal-specific PCR primers developed for analysis of the ITS region of environmental DNA extracts. *BMC Microbiology*, 5(1), 28.
- Martínez-Pérez, C., Greening, C., Bay, S.K., Lappan, R.J., Zhao, Z., De Corte, D. et al. (2022) Phylogenetically and functionally diverse microorganisms reside under the Ross Ice Shelf. *Nature Communications*, 13(1), 117.
- McCormack, M.L., Dickie, I.A., Eissenstat, D.M., Fahey, T.J., Fernandez, C.W., Guo, D. et al. (2015) Redefining fine roots improves understanding of below-ground contributions to terrestrial biosphere processes. *New Phytologist*, 207(3), 505–518.
- McKnight, D.T., Huerlimann, R., Bower, D.S., Schwarzkopf, L., Alford, R.A. & Zenger, K.R. (2019) Methods for normalizing microbiome data: an ecological perspective. *Methods in Ecology and Evolution*, 10(3), 389–400.
- McMurdie, P.J. & Holmes, S. (2013) phyloseq: an R package for reproducible interactive analysis and graphics of microbiome census data. *PLoS One*, 8(4), e61217.
- Midgley, M.G., Brzostek, E. & Phillips, R.P. (2015) Decay rates of leaf litters from arbuscular mycorrhizal trees are more sensitive to soil effects than litters from ectomycorrhizal trees. *Journal of Ecology*, 103(6), 1454–1463.
- Minerovic, A.J., Valverde-Barrantes, O.J. & Blackwood, C.B. (2018) Physical and microbial mechanisms of decomposition vary in importance among root orders and tree species with differing chemical and morphological traits. *Soil Biology and Biochemistry*, 124, 142–149.
- Nakayasu, E.S., Nicora, C.D., Sims, A.C., Burnum-Johnson, K.E., Kim, Y.-M., Kyle, J.E. et al. (2016) MPEX: a robust and universal protocol for single-sample integrative proteomic, metabolomic, and lipidomic analyses. *mSystems*, 1(3), e00043–00016.
- Nordin, A. & Näsholm, T. (1997) Nitrogen storage forms in nine boreal understory plant species. *Oecologia*, 110(4), 487–492.
- Oksanen, J., Blanchet, F.G., Kindt, R., Legendre, P., Minchin, P., O'Hara, B. et al. (2015) Vegan: community ecology package. *R Package Version 2.2-1*, 2, 1–2.
- Parada, A.E., Needham, D.M. & Fuhrman, J.A. (2016) Every base matters: assessing small subunit rRNA primers for marine microbiomes with mock communities, time series and global field samples. *Environmental Microbiology*, 18(5), 1403–1414.
- Peiffer, J.A., Spor, A., Koren, O., Jin, Z., Tringe, S.G., Dangl, J.L. et al. (2013) Diversity and heritability of the maize rhizosphere microbiome under field conditions. *Proceedings of the National Academy of Sciences*, 110(16), 6548–6553.
- Pregitzer, K.S., DeForest, J.L., Burton, A.J., Allen, M.F., Ruess, R.W. & Hendrick, R.L. (2002) Fine root architecture of nine North American trees. *Ecological Monographs*, 72(2), 293–309.
- Quast, C., Pruesse, E., Yilmaz, P., Gerken, J., Schweer, T., Yarza, P. et al. (2013) The SILVA ribosomal RNA gene database project: improved data processing and web-based tools. *Nucleic Acids Research*, 41, 590–596.
- R Core Team (2012). R: A language and environment for statistical computing. R Foundation for Statistical Computing.
- Reinhold-Hurek, B., Büniger, W., Burbano, C.S., Sabale, M. & Hurek, T. (2015) Roots shaping their microbiome: global hotspots for microbial activity. *Annual Review of Phytopathology*, 53(1), 403–424.
- Schreiter, S., Ding, G.-C., Heuer, H., Neumann, G., Sandmann, M., Grosch, R. et al. (2014) Effect of the soil type on the microbiome in the rhizosphere of field-grown lettuce. *Frontiers in Microbiology*, 5(144), 144.
- Segal, E., Kushnir, T., Mualem, Y. & Shani, U. (2008) Water uptake and hydraulics of the root hair rhizosphere. *Vadose Zone Journal*, 7(3), 1027–1034.
- Shaffer, M., Borton, M.A., McGivern, B.B., Zayed, A.A., La Rosa, S.L., Solden, L.M. et al. (2020) DRAM for distilling microbial metabolism to automate the curation of microbiome function. *Nucleic Acids Research*, 48(16), 8883–8900.
- Sharma, B. & Ahlert, R.C. (1977) Nitrification and nitrogen removal. *Water Research*, 11(10), 897–925.

- She, W., Bai, Y., Zhang, Y., Qin, S., Feng, W., Sun, Y. et al. (2018) Resource availability drives responses of soil microbial communities to short-term precipitation and nitrogen addition in a desert shrubland. *Frontiers in Microbiology*, 9, 186.
- Tkacz, A., Bestion, E., Bo, Z., Hortala, M. & Poole, P.S. (2020) Influence of plant fraction, soil, and plant species on microbiota: a multikingdom comparison. *mBio*, 11(1), e02785–02719.
- Valenzuela-Estrada, L.R., Vera-Caraballo, V., Ruth, L.E. & Eissenstat, D.M. (2008) Root anatomy, morphology, and longevity among root orders in *Vaccinium corymbosum* (Ericaceae). *American Journal of Botany*, 95(12), 1506–1514.
- Weiss, S., Xu, Z.Z., Peddada, S., Amir, A., Bittinger, K., Gonzalez, A. et al. (2017) Normalization and microbial differential abundance strategies depend upon data characteristics. *Microbiome*, 5(1), 27.
- Winter, G., Todd, C.D., Trovato, M., Forlani, G. & Funck, D. (2015) Physiological implications of arginine metabolism in plants. *Frontiers in Plant Science*, 6, 534.
- Yates, C.F., Guo, J., Bell, T.H., Fleishman, S.M., Bock, H.W., Trexler, R.V. et al. (2021) Tree-induced alterations to soil properties and rhizosphere-associated bacteria following 23 years in a common garden. *Plant and Soil*, 461, 591–602.
- Zhang, Y., Xu, J., Riera, N., Jin, T., Li, J. & Wang, N. (2017) Huanglongbing impairs the rhizosphere-to-rhizosphere

enrichment process of the citrus root-associated microbiome. *Microbiome*, 5(1), 97.

- Zhong, Y., Sorensen, P.O., Zhu, G., Jia, X., Liu, J., Shanguan, Z. et al. (2022) Differential microbial assembly processes and co-occurrence networks in the soil-root continuum along an environmental gradient. *iMeta*, 1, e18.

SUPPORTING INFORMATION

Additional supporting information can be found online in the Supporting Information section at the end of this article.

How to cite this article: King, W.L., Yates, C.F., Cao, L., O'Rourke-Ibach, S., Fleishman, S.M., Richards, S.C. et al. (2023) Functionally discrete fine roots differ in microbial assembly, microbial functional potential, and produced metabolites. *Plant, Cell & Environment*, 46, 3919–3932. <https://doi.org/10.1111/pce.14705>